Manganese doped bismuth vanadate solid electrolytes: oxygen permeation in $Bi_2V_{0.8}Mn_{0.2}O_{5.3}$

Y. L. Yang, L. Qiu and A. J. Jacobson*

Department of Chemistry, University of Houston, Houston, TX 77204–5641, USA

Oxygen permeation and transference number measurements have been made on dense membranes of $Bi_2V_{0.8}Mn_{0.2}O_{5.3}$. Measurements of the permeation flux as a function of membrane thickness and oxygen partial pressure gradient suggest that the oxygen transport is limited by bulk diffusion rather than by surface exchange kinetics. The electronic conductivity of the sample at 750–850 °C was obtained from the permeation flux measurements and found to be in the range 2×10^{-3}–10^{-2} S cm^{-1}. The transference numbers were measured by a potentiometric technique in two oxygen partial pressure gradients. The values range from 0.67 at 550 °C to 0.82 at 850 °C. At high temperature, the transference numbers measured by the potentiometric technique are in close agreement with those derived from the permeation flux and the total electrical conductivity data. At lower temperatures, the results are significantly different, most likely due to slow electrode kinetics.

Oxygen permeation through a dense oxide membrane is a direct indication of the existence of mixed ionic and electronic conductivity in the membrane material. Permeation measurements on mixed conducting membranes have been reported recently for a number of perovskite oxides[1–4] and for several stabilized bismuth oxides, for example, $(Bi_2O_3)_{0.85}(La_2O_3)_{0.15}$,[5] $(Bi_2O_3)_{0.75}(Er_2O_3)_{0.25}$,[6] and $(Bi_2O_3)_{0.60}(Tb_2O_3)_{0.40}$.[7] Detailed studies of the surface exchange kinetics and of the control of the bulk transport by the electronic conductivity have been reported for some of the materials.[6,7] Partial substitution of vanadium by other metals in $Bi_2VO_{5.5}$ leads to a series of compositions often referred to as the BIMEVOX phases which have high conductivity that is predominantly ionic.[8] Iharada *et al.*[9] showed by using a potentiometric technique to determine transference numbers that the electronic contributions to the conductivities of the Cu and Ni substituted phases are significant. Measurements of the p_{O_2} dependence of the total conductivity also indicate that the doped $Bi_2VO_{5.5}$ phases are mixed conductors.[9,10] To our knowledge, no oxygen permeability measurements have been reported for the BIMEVOX phases.

In two previous papers, we reported the synthesis and characterization of manganese doped bismuth vanadates, $Bi_2V_{1-x}Mn_xO_{5.5-x}$ $(0.1 \leqslant x \leqslant 0.25)$,[11] and measurements of their total electrical conductivities by using ac impedance spectroscopy.[12] The Mn dopant was shown by magnetic measurements to be in the 3+ oxidation state at low temperatures but is partially reduced to the 2+ oxidation state at high temperatures.[11] The total electrical conductivity of the oxides increases as p_{O_2} is reduced, suggesting that the materials have some mixed conductivity. In the present paper, we report oxygen permeation measurements for one particular composition: $Bi_2V_{0.8}Mn_{0.2}O_{5.3}$. Transference numbers as a function of temperature were also measured for the same composition using a potentiometric method. These values are compared with the corresponding data obtained from an analysis of the permeation results.

Experimental

A polycrystalline sample of $Bi_2V_{0.8}Mn_{0.2}O_{5.3}$ was synthesized according to the anneal–melt–quench procedure reported previously.[11] The powder sample was ground in an agate mortar with acetone for 1 h before it was used to press discs. Disc membranes were obtained by uniaxial pressing at 25 000 psi. In the fabrication of some discs, small amounts of gold powder (Refining Systems, 3–5 μm) were added to improve the sintering and mechanical properties. It was much easier to produce high-temperature seals with the gold-modified discs (see below). The discs were sintered at 870 °C for 5 h. The heating and cooling rates were 2 °C min^{-1}. The diameters of the sintered discs were approximately 12.4 mm. At the end of the processing, the disc density was determined by measuring the dimensions and total mass of the disc. The final density was approximately 90–92% of the theoretical density calculated assuming the tetragonal unit cell dimensions of $Bi_2V_{0.8}Mn_{0.2}O_{5.3}$[11] and the amount of gold added. As a final step, both surfaces of the discs were ground using 600 grit SiC polishing paper, and further polished to a 6 μm finish using diamond paste.

The oxygen permeation fluxes were measured using an apparatus described previously.[4] A disc membrane sandwiched between two gold rings is held in place by two quartz tubes. The gold rings are approximately 2.0 mm wide, leaving an effective area for oxygen permeation of approximately 0.49 cm^2. The whole assembly is supported by a larger quartz tube. Four screws at one end of the assembly are used to adjust the pressure exerted on the gold rings to ensure gas-tightness at both sides of the disc membrane. Springs are loaded at the other end of the assembly so that mechanical strains can be relieved without breaking the quartz tubes. Mixtures of oxygen and nitrogen are fed into one side (the oxygen-rich side) of the apparatus, while helium gas with a typical flow rate of 20 cm^3 min^{-1} is swept through the other side (the oxygen-lean side). The oxygen partial pressures on the oxygen-rich side were varied between 0.15 and 1 atm. An MTI M200 gas chromatograph equipped with an automated sampling pump and a molecular sieve column for separation of oxygen and nitrogen is connected to the exit of the sweeping gas to measure both oxygen and nitrogen concentrations. The gas chromatograph was frequently calibrated using a standard gas mixture of oxygen and nitrogen in helium balance. The permeation assembly was placed in a single-zone furnace equipped with a ATS 3210 temperature controller. The disc temperature was more accurately monitored by an inserted thermocouple. At each temperature, the oxygen permeation flux was periodically measured until a constant flux was obtained. The permeation fluxes reported below are the steady state values.

The apparatus used for the potentiometric measurements was similar to that used for the permeation measurements with minor modifications to accommodate electrical leads in contact with each side of the membrane. The centres of both sides of the membrane (1.0 mm thickness) were painted with

Engelhard 6924 Pt paste and then activated at 750 °C to form electrodes. The platinum electrodes on each side covered an area of approximately 0.15 cm^2, making them quasi-large area electrodes.[9] A pair of Pt electrical leads supported in alumina tubes were pressed onto the disc electrodes by a spring-loading mechanism. Oxygen and nitrogen gas mixtures of known concentrations were swept over both sides of the membrane to create a fixed oxygen partial pressure gradient. Voltages between the two electrodes were measured by using a high impedance Keithley 617 electrometer.

Results

From the oxygen concentrations in the helium gas and the helium flow rate, the total oxygen permeation rates (mol s^{-1}) were calculated assuming the ideal gas law. Any small oxygen leakages due to pin-holes or cracks on the disc were monitored by measuring the concentration of nitrogen in the helium sweep gas. The oxygen fluxes were then corrected for oxygen leakage using the corresponding nitrogen concentrations. Corrections were typically $<3\%$ of the total oxygen flux for the composite membranes. For the pure oxide membranes, the leak rates were somewhat higher ($\leqslant 10\%$). The permeation fluxes (mol cm^{-2} s^{-1}) were calculated by dividing the permeation rates by the effective surface area of the discs. The transference numbers were determined from the ratio of the measured open circuit voltages at a fixed temperature and oxygen partial pressure gradient to the corresponding theoretical values calculated from the Nernst equation.

The time-dependent behaviour of the oxygen permeation flux is shown in Fig. 1. The membrane used in the experiments contained 9 vol.% gold and was 1.0 mm thick. The helium flow rate was fixed at 20 cm^3 min^{-1}. The data shown as filled and open circles were obtained when the temperature was stepped up from 750 to 760 °C and down from 753 to 740 °C, respectively. The oxygen partial pressures on the oxygen-rich and the oxygen-lean sides were 0.20 atm and approximately 3.5×10^{-4} atm. In response to the temperature change, the initial value of the flux was observed to relax to the steady state value in *ca.* 20 min. This equilibration time is much faster than observed in similar measurements with $SrCo_{0.8}Fe_{0.2}O_{3-\delta}$.[4]

Fig. 2 shows a comparison of the permeation flux through membranes with and without added gold. The two membranes were each 1.0 mm thick with gold contents of 0 and 9 vol.%, respectively. The flux data were taken on cooling after the discs had first been annealed at high temperature. The pure oxide disc had rather significant leakage below 780 °C ($\leqslant 10\%$ of the total flux), while the gold-modified discs had much smaller leakage ($<3\%$). Within the experimental error, the flux data for the membrane containing 9 vol.% gold are almost identical to that for the pure oxide membrane. The apparent activation energies are approximately 67 kJ mol^{-1} for discs of pure $Bi_2V_{0.8}Mn_{0.2}O_{5.3}$ and with 9 vol.% gold.

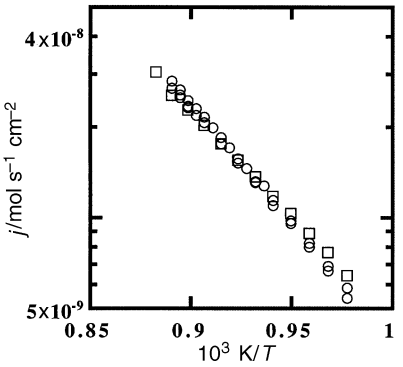

Fig. 2 Dependence of the oxygen permeation flux on temperature for membranes with 0 vol.% (□) and 9 vol.% (○) gold. Both membranes are 1.0 mm thick and $p_{O_2}^{rich} = 0.20$ atm.

A significant hysteresis effect was observed in the permeation measurements as indicated by the data shown in Fig. 3. The membrane used in these measurements was identical to the one used in the time-dependent measurements shown in Fig. 1 and the oxygen partial pressures were $p_{O_2}^{rich} = 0.20$ atm and $p_{O_2}^{lean} = 10^{-4}$–10^{-3} atm. The permeation flux data obtained by first annealing the disc at 850 °C and then making the flux measurements on cooling show Arrhenius behaviour. Significant deviations from Arrhenius behaviour at temperatures <750 °C, however, are apparent in data measured on heating after the membrane had been annealed at 680 or 450 °C for 3 h. At temperatures >750 °C, the flux data converge and no hysteresis effect can be seen. Similar hysteresis effects were observed in measurements of the total electrical conductivity.[12]

The permeation data for two membranes with thicknesses of 1.0 and 2.0 mm are shown in Fig. 4. The gold content was 9 vol.% for both membranes. The oxygen partial pressure at the oxygen rich side was fixed at 0.20 atm in both measurements. The flux measurements were made on cooling after the discs had first been annealed at 850 °C. The oxygen permeation fluxes are approximately proportional to the inverse of the disc thickness at high temperature. However, at low temperature, the flux data show significant deviations from this relationship (see below).

The oxygen permeation data in different oxygen partial pressure gradients are shown in Fig. 5. In these experiments, the membrane used was 1.0 mm thick and contained 9 vol.% gold. Various oxygen partial pressures in the range 0.15 atm $\leqslant p_{O_2}^{rich} \leqslant$ 1.0 atm were obtained by mixing oxygen and nitrogen gases. The lowest partial pressure used was 0.15 atm chosen

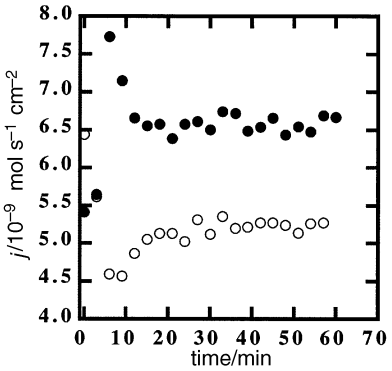

Fig. 1 Time dependence of the oxygen permeation flux. ●, Temperature changed from 750 to 760 °C; ○, temperature changed from 753 to 740 °C

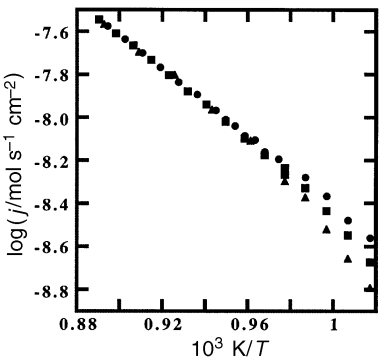

Fig. 3 Hysteresis effects on the oxygen permeation flux. ●, Membrane annealed at 850 °C and *j* measured on cooling; membrane annealed at 680 °C (■) and at 450 °C (▲), respectively, *j* measured on heating.

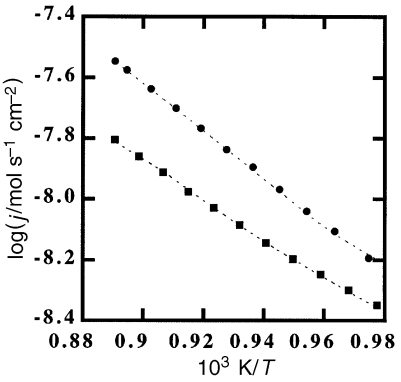

Fig. 4 Thickness dependence of the oxygen permeation fluxes for composite membranes containing 9 vol.% gold, $p_{O_2}^{rich}=0.20$ atm. ●, $l=1.0$ mm; and ■, $l=2.0$ mm. The dotted lines are fits to the measured data.

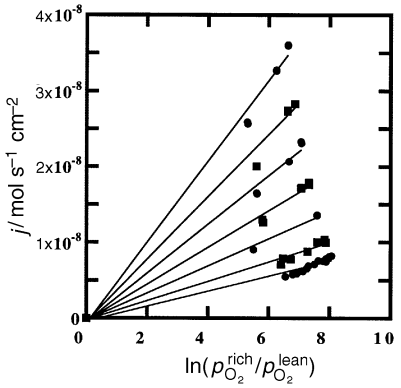

Fig. 5 The dependence of the flux on the oxygen partial pressure gradient for a 9 vol.% gold-containing membrane 1 mm thick

to minimize effects on the data due to permeation through the membrane edge (see below). $p_{O_2}^{lean}$ ranged from 2.2×10^{-4} to 1.3×10^{-3} atm. The permeation flux increases linearly with the log of the oxygen partial pressure gradient at the selected temperatures. The linear fits to the data were constrained to pass through the origin.

The transference numbers were measured at two different oxygen partial pressure gradients: (1) $p_{O_2}^{rich}=0.194$ atm and $p_{O_2}^{lean}=0.0102$ atm and (2) $p_{O_2}^{rich}=1.0$ atm and $p_{O_2}^{lean}=0.203$ atm in the temperature range 550–850 °C. The transference numbers are summarized in Fig. 6. Under the two sets of conditions, essentially identical (±1%) transference numbers were

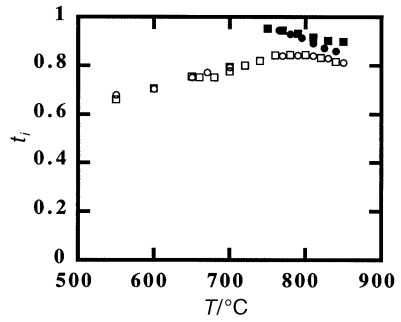

Fig. 6 The transference number, t_i, for a composite membrane containing 9 vol.% gold. Data from open circuit voltage measurements are shown as open symbols: □, $p_{O_2}^{rich}=1.0$ atm and $p_{O_2}^{lean}=0.21$ atm; ○, $p_{O_2}^{rich}=0.194$ atm and $p_{O_2}^{lean}=0.0102$ atm. Data from permeation measurements are shown as solid symbols: ●, calculated from the slopes of the gradient-dependent flux curves in Fig. 5 and the total conductivity; ■, calculated from the diffusion coefficient data in Fig. 7 and the total conductivity.

obtained. The transference numbers range from 0.67 to 0.85. The values are smaller at lower temperature and increase with temperature, reaching a maximum at approximately 800 °C.

Discussion

The observed oxygen permeation fluxes, the measured transference numbers and the pressure dependence of the total electrical conductivity[11] indicate that BIMNVOX oxides are mixed conductors under our experimental conditions. Electronic conductivity has previously been reported in other BIMEVOX systems.[9,10]

The dependence of the permeation flux on the membrane thickness is shown in Fig. 4. At high temperature, the fluxes are approximately proportional to the inverse of the membrane thickness, suggesting that the rate-limiting step is bulk diffusion. The dependence of the flux on the log of partial pressure gradient (Fig. 5) also supports this conclusion. Significant deviations from the Wagner equation are observed, however, at low temperatures due to oxygen permeation through the edge of the membrane. The effect of edge permeation is small when the permeation is limited by bulk diffusion as is the case here but is sufficient to account for the observed deviation. We have developed a model to correct the data for the effects of edge permeation in the general case where the oxygen permeation rate is determined by both surface exchange and bulk diffusion.[13] In this model, the flux of oxygen ions across the interfaces ($j_{interface}$) is expressed as

$$j_{interface}=c_i k\,[\exp(\mu_g/RT)-\exp(\mu/RT)] \quad (1)$$

and the oxygen ion flux in the bulk (j_{bulk}) as:

$$j_{bulk}=-\frac{c_i D_a}{RT}\nabla\mu \quad (2)$$

where c_i is the concentration of oxygen ions in the solid, μ_g and μ are the chemical potentials of oxygen atoms in the gas and in the solid phases, respectively and $\Delta\mu$ is the oxygen chemical potential gradient across the membrane. Two parameters, D_a the ambipolar diffusion coefficient and k the surface exchange coefficient, are used to characterize the permeation behaviour. The ratio $D_a/k=L_d$ defines a characteristic length scale for the transition from bulk to surface limitated transport. When the membrane thickness $l\gg L_d$, the permeation process is limited by bulk diffusion and when $l\ll L_d$, the permeation process is limited by the surface exchange rate. The two equations given above can be solved numerically by matching the oxygen ion flux across the interfaces with the ion flux in the bulk solid and using the appropriate boundary conditions. The model is described in detail in ref. 13. Numerical simulation of the permeation data with this model yielded an excellent fit to the data as indicated by the calculated values (dotted lines) shown in Fig. 4. The values of k and D_a determined from the simulation are shown in Fig. 7. The activation energies are 90.7 and 65.2 kJ mol^{-1} for surface exchange and bulk diffusion, respectively. The value of L_d increases from 6.8×10^{-4} cm at 850 °C to 1.1×10^{-3} cm at 750 °C. The increase in L_d explains the significant upward deviation of the data in Fig. 4 at low temperatures for the thicker membrane. The edge contributions to the oxygen flux are *ca.* 10 and *ca.* 28% for the 1.0 and 2.0 mm thick membranes, respectively.

Ignoring the relatively small contribution from edge permeation for the 1 mm thick membrane and recognizing that the small value of L_d indicates that bulk diffusion dominates the overall permeation process, the bulk electronic conductivity, σ_e, can be calculated by using the Wagner equation and the data in Fig. 5.[5]

$$j=\frac{RT}{4^2F^2l}\frac{\sigma_e(\sigma_{total}-\sigma_e)}{\sigma_{total}}\ln\frac{p^{rich}}{p^{lean}}$$

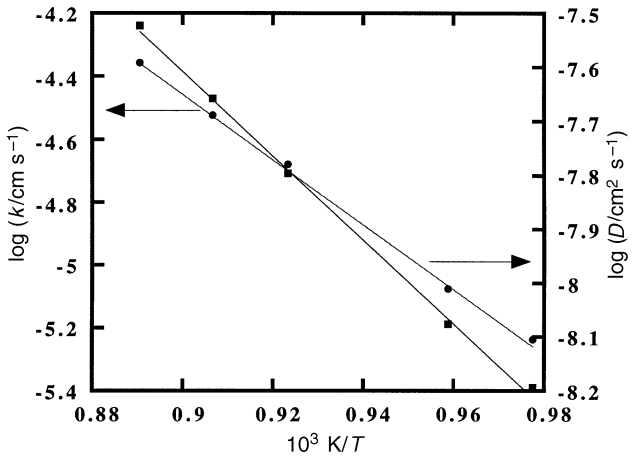

Fig. 7 Bulk diffusion and surface exchange coefficients derived from the numerical simulation of the thickness-dependent permeation flux data in Fig. 4

where R is the gas constant, T the temperature, F the Faraday constant, l the membrane thickness, σ_e the electronic conductivity and σ_{total} the total electrical conductivity. At temperatures $<790\,^{\circ}C$, the measured total electrical conductivity data[12] were used in the calculation. At temperatures $>790\,^{\circ}C$, the electrical conductivity data were extrapolated from the measured data. The electronic conductivity derived in this way is shown as a function of temperature in Fig. 8. The electronic conductivity calculated from the diffusion coefficients given in Fig. 7 by using the Nernst–Einstein equation are also presented in Fig. 8. The results obtained by the two different methods are in quite good agreement. The small discrepancy between the two estimates that is noticeable at the higher temperatures may be due to uncertainties introduced by using extrapolated values for the total conductivity. It is also possible that the difference arises from the neglect of edge permeation in the estimate from the Wagner equation. The edge effect is properly accounted for in the estimate from the diffusion coefficients.

The ionic transference number at various temperatures can be calculated from the electronic and the total electrical conductivity.[12] The transference numbers calculated in this way are shown as the solid symbols in Fig. 6. Again the total electrical conductivity data at temperatures $>790\,^{\circ}C$ are extrapolated values and have some uncertainties. Nevertheless, it is apparent in Fig. 6 that the average transference numbers at high temperatures measured by the potentiometric technique are very similar to the values derived from the permeation flux data. But at temperature $<830\,^{\circ}C$, the measured values are significantly lower than the calculated transference number

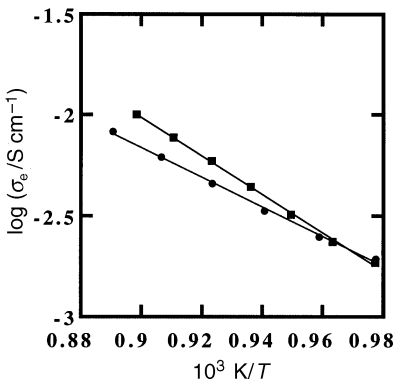

Fig. 8 Electronic conductivity *vs.* reciprocal temperature. ■, Calculated from the gradient-dependent permeation flux data; ●, calculated from the diffusion coefficients.

data. The difference in the two sets of transference numbers is most likely due to interfacial polarization between the Pt electrodes and the BIMNVOX membrane. Kleitz *et al.*[14,15] and Liu and Hu[16] have discussed such departures from the ideal Nernst behaviour. Experimentally, the deviation of the transference numbers measured by potentiometric techniques from values derived by using other methods has been observed in a number of mixed conducting oxides, such as BICUVOX,[9] doped CeO_2,[17] and very recently $BaCe_{0.8}Gd_{0.2}O_3$.[18] In general, deviations arise from slow electrode kinetics at the electrode membrane interface and are expected to be larger at lower temperatures. Such deviations at lower temperatures have been reported previously[9,17,18] and are observed in the present system.

Finally, the transference numbers of $Bi_2V_{0.8}Cu_{0.2}O_{5.2}$ measured by the potentiometric technique[9] are compared with those of $Bi_2V_{0.8}Mn_{0.2}O_{5.3}$. With quasi-large area electrodes under an oxygen pressure gradient corresponding to $p_{O_2}^{rich}=1.0$ atm and $p_{O_2}^{lean}=0.2$ atm, the average transference numbers at 744 °C are 0.86 and 0.83 for BICUVOX and BIMNVOX, respectively, and at 591 °C the respective numbers are 0.70 and 0.69. The closely similar transference numbers indicate that the dopant transition metal has little effect on the electrode interfacial polarization process.

Conclusion

The solid solution $Bi_2Mn_{0.2}V_{0.8}O_{5.3}$ has been shown to have electronic conductivity by oxygen permeation and potentiometric measurements. The variations of the oxygen permeation flux with membrane thickness and oxygen partial pressure gradient indicate that bulk diffusion dominates the overall permeation rate. The measured permeation flux is significantly lower than observed in perovskite structure oxides, for example, $SrCo_{0.8}Fe_{0.2}O_{3-x}$, under similar conditions. The electronic conductivity was derived from the permeation flux results. The transference numbers obtained from the permeation flux and the total electrical conductivity are in agreement with the potentiometric measurements at high temperature. Significant discrepancies are observed at low temperatures and are due to slow electrode kinetics.

We thank the Robert A. Welch Foundation and Texas Center for Superconductivity for financial support of this work. This work was supported in part by the MRSEC program of the National Science Foundation under Award Number DMR-9632667.

References

1 Y. Teraoka, H. Zhang, S. Furukawa and N. Yamazoe, *Chem. Lett.*, 1985, 1743.
2 Y. Teraoka, H. Zhang, K. Okamoto and N. Yamazoe, *Mater. Res. Bull.*, 1988, **23**, 51.
3 H. Kruidhof, H. J. M. Bouwmeester, R. H. E. v. Doorn and A. J. Burggraaf, *Solid State Ionics*, 1993, **63–65**, 816.
4 L. Qiu, T. H. Lee, L.-M. Liu, Y .L. Yang and A. J. Jacobson, *Solid State Ionics*, 1995, **76**, 321.
5 R. D. Cosimo, J. D. Burrington and R. K. Grasselli, *J. Catal.*, 1986, **102**, 234.
6 H. J. M. Bouwmeester, H. Kruidhof, A. J. Burggraaf and P. J. Gellings, *Solid State Ionics*, 1992, **53–56**, 460.
7 H. J. M. Bouwmeester, H. Kruidhof and A. J. Burggraaf, *Solid State Ionics*, 1994, **72**, 185.
8 F. Abraham, J. C. Boivin, G. Mairesse and G. Nowogrocki, *Solid State Ionics*, 1990, **40–41**, 934.
9 T. Iharada, A. Hammouche, J. Fouletier, M. Kleitz, J. C. Boivin, and G. Mairesse, *Solid State Ionics*, **48**, 1991, 257.
10 J. G. Goodenough, A. Manthiram, M. Paranthaman and Y. S. Zhen, *Solid State Ionics*, 1992, **52**, 105.
11 Y. L. Yang, L. Qiu, W. T. A. Harrison, R. Christoffersen and A. J. Jacobson, *J. Mater. Chem.*, 1997, **7**, 243.

12 L. Qiu, Y. L. Yang and A. J. Jacobson, *J. Mater. Chem.*, 1997, **7**, 249.
13 T. H. Lee, Y. L. Yang, A. J. Jacobson, B. Abeles and M. Zhou, *Solid State Ionics*, in press.
14 M. Kleitz, E. Siebert and J. Fouletier, in *Chemical Sensors*, ed. T. Seiyama, K. Fueki, J. Shiokawa and S. Suzuki, Kodansha/Elsevier, Tokyo, 1983, p.262.
15 M. Kleitz and E. Siebert, in *Chemical Sensor Technology*, ed. T. Seiyama, Kodansha, Tokyo, 1989, vol. 2, p.151.
16 M. Liu, in *Proceedings of the First International Symposium on Ionic and Mixed Conducting Ceramics*, ed. T. A. Ramanarayanan and H. L. Tuller, The Electrochemical Society, Pennington, NJ, 1991, PV91–12, p.191.
16 J. Fouletier and M. Henault, *Solid State Ionics*, 1983, **9–10**, 1277.
17 M. Liu and H. Hu, *J. Electrochem. Soc.*, 1996, **143**, L109.

Paper 6/07800A; *Received* 18*th November*, 1996